Simulating Solute Transport Across Horizontal-Flow Barriers Using the MODFLOW Ground-Water Transport Process

By G.Z. Hornberger, L.F. Konikow, and P.T. Harte

U.S. DEPARTMENT OF THE INTERIOR
GALE NORTON, Secretary

U.S. GEOLOGICAL SURVEY
Charles G. Groat, Director

CONTENTS

TABLES

FIGURES

PREFACE

This report describes modifications to a three-dimensional solute-transport model (*MODFLOW-GWT*) developed by the U.S. Geological Survey (USGS). The modifications improve the capability of *MODFLOW-GWT* to accurately simulate transport in models that use the Horizontal-Flow Barrier (HFB) Package in MODFLOW. The updated code (1) allows the user to input dispersivity and diffusion properties of HFB barriers, and (2) modifies the calculation of dispersive solute flux near barriers.

The code and documentation for this model are available for downloading over the Internet from a USGS software repository. The repository is accessible from a Web site for USGS ground-water models at **http://water.usgs.gov/nrp/gwsoftware/**. When this code is revised or updated in the future, new versions or releases will be made available for downloading from this same site.

Although extensive testing of the modifications of the code indicates that this model will yield reliable calculations for a variety of field problems, the user is cautioned that the accuracy of the model can be affected appreciably for certain combinations of parameter values.

Simulating Solute Transport Across Horizontal-Flow Barriers Using the MODFLOW Ground-Water Transport Process

by   George Z. Hornberger
Leonard F. Konikow
Philip T. Harte

ABSTRACT

This report describes modifications to a U.S. Geological Survey (USGS) three-dimensional solute-transport model (*MODFLOW-GWT*), which is incorporated into the USGS *MODFLOW* ground-water model as the Ground-Water Transport (GWT) Process. The modifications improve the capability of *MODFLOW-GWT* to accurately simulate solute transport in simulations that use the Horizontal-Flow Barrier (HFB) Package in *MODFLOW*. The updated code (called the CHFB Package) (1) allows the user to input dispersivity and diffusion properties of HFB barriers, and (2) modifies the calculation of dispersive solute flux near barriers.

The Horizontal-Flow Barrier Package of the *MODFLOW* model is a valuable tool for simulating ground-water flow through aquifers containing either natural or artificial low-permeability vertical features. A modification to the Ground-Water Transport (GWT) Process that is compatible with the HFB package has been developed and tested. When HFB is active, the consideration of advective solute flux is straightforward. The consideration of dispersive solute flux is more problematic because the standard evaluation of the cross-product terms of the dispersion tensor in the finite-difference grid may require the estimation of concentration gradients using nodal values on both sides of the barrier. This standard evaluation may be a poor estimator of concentration gradients at a point on one side of the barrier, however, if the concentrations (and concentration gradients) differ greatly on the other side of the barrier--a condition that would be expected for a barrier constructed to contain contaminated ground water. Therefore, this condition could lead to inaccurate estimates of solute flux attributable to the cross-product terms of the dispersion tensor. Thus, for grid locations near a horizontal-flow barrier, the standard finite-difference approximation was modified so that specific components of the concentration gradients for the cross-product terms are calculated over a distance of one cell rather than over two cells. In addition, the CHFB Package allows the dispersive properties of the barrier to have different values than those of the aquifer. Evaluation of numerical experiments indicates that the CHFB Package yields improved results.

INTRODUCTION

Low-permeability, non-reactive, horizontal-flow barrier walls are used to contain contaminants in an aquifer and prevent their further spreading into ground water. Although barriers typically are constructed of much lower-permeability material than the surrounding aquifer, most barriers are not impermeable and solute transport occurs through them, although at rates that are much slower than rates of solute

transport in the aquifer. The presence of features such as low-permeability barriers may strongly affect head distributions and ground-water flow, and similarly will affect solute transport and concentration distributions.

Accurate computation of rates of solute transport through a barrier wall is important for evaluating remedial activities and estimating the time needed to restore an aquifer. Two main numerical simulation approaches can be used to simulate horizontal barriers. In one approach, the hydraulic properties and physical dimensions of the barrier are represented explicitly by the properties assigned to the grid cells coinciding with the location of the barrier within the aquifer domain. Barriers usually are narrow (on the order of several feet) relative to the scale of a simulated ground-water flow system (which may be on the order of miles). Therefore, this approach may require the use of a very fine grid that may be computationally intensive and inefficient. In the second approach, the hydraulic properties of the barrier are represented implicitly by adjusting the inter-cell hydraulic conductance for cell faces coinciding with the barrier location so that they represent barrier properties (adjacent cells are assigned aquifer properties). This implicit representation is suitable when the barrier width is negligibly small relative to the horizontal dimensions of cells in the grid. The implicit technique has been described by Hsieh and Freckleton (1993) and has the advantage that it does not require fine discretization of the model to accommodate the dimensions and properties of the barrier.

Neville and others (1998) noted deficiencies in numerical modeling of solute transport through implicitly represented low-permeability features, including horizontal-flow barriers formed by constructed slurry walls. The results of their numerical experiments comparing explicit and implicit representations indicated that the implicit representation yielded premature breakthrough and solute flux rates through the barrier that were erroneously too high. They attributed these errors to the advection process because the barrier width is assumed to be infinitesimally small. Thus, the implicit representation inherently is unable to simulate either solute storage or transport distance and travel time in the barrier. This study examines whether some of the error also is related to the dispersion process. The numerical experiments and analysis of Neville and others (1998) assumed uniform dispersive transport properties (that is, the same dispersivities and effective diffusion coefficients apply to transport across the barrier as to transport through the aquifer). In this study, whether removal of this restrictive assumption can improve the numerical results is examined. Also, because of concerns about the accuracy of the standard finite-difference algorithm used to calculate dispersive flux, a new approach for calculating dispersive flux in cells near barriers is introduced and evaluated.

This study aims to develop a reliable means to simulate solute transport through horizontal-flow barriers when the ground-water flow equation is solved using an implicit representation of the barrier. Numerical simulation tests were used to help understand the effect of alternative simulation techniques on advective and dispersive solute transport adjacent to and through a low-permeability, non-reactive barrier wall. The purpose of this report is to describe the results of this study. The ground-water-flow and solute-transport models are described. Numerical experiments using the models are described, and input and output instructions for the CHFB Package and sample problem are given.

GROUND-WATER-FLOW MODEL

MODFLOW is a commonly used model for simulating three-dimensional ground-water-flow systems. Comprehensive documentation of *MODFLOW* is presented by McDonald and Harbaugh (1988), Harbaugh and McDonald (1996), and Harbaugh and others (2000). *MODFLOW* uses implicit (backward-in-time) finite-difference methods to numerically solve the governing three-dimensional ground-water-flow equation. The fluid flux between two nodes (that is, across a cell face) is computed on the basis of the hydraulic conductance and the difference in head between those two nodes. The hydraulic conductance between the two cells is related to the distance between adjacent nodes and some user-specified averaging scheme (a common one being the harmonic mean) for the hydraulic conductivity.

The method developed by Hsieh and Freckleton (1993) allows *MODFLOW* to more efficiently simulate thin, vertical, low-permeability geologic or artificial features that impede horizontal flow of ground water. The method was incorporated into *MODFLOW* as an optional Horizontal-Flow Barrier (HFB) package. The vertical features are approximated by assigning appropriately low hydraulic conductance values to the face between two contiguous model cells. Because the method directly modifies the inter-cell hydraulic conductance, the barrier width is not explicitly represented in the solution. The key assumptions are that the width of the barrier is negligibly small relative to horizontal spacing of the adjacent model cells and that there is no storage capacity within the barrier materials.

SOLUTE-TRANSPORT MODEL

The Ground-Water Transport (GWT) Process is an optional package for *MODFLOW* that solves the three-dimensional solute-transport equation; it is based on the *MOC3D* model (Konikow and others, 1996). The solute-transport equation may be written as

$$\frac{\partial C}{\partial t} + \frac{V_i}{R_f}\frac{\partial C}{\partial x_i} - \frac{1}{\varepsilon R_f}\frac{\partial}{\partial x_i}\left(\varepsilon D_{ij}\frac{\partial C}{\partial x_j}\right) - \frac{\sum[W(C'-C)]}{\varepsilon R_f} + \lambda C = 0, \qquad (1)$$

where C is concentration (ML^{-3}), ε is effective porosity (dimensionless), V is interstitial fluid velocity (LT^{-1}), D is a second-rank tensor of dispersion coefficients (L^2T^{-1}), W is a volumetric fluid sink or source rate per unit volume of aquifer (T^{-1}), C' is the concentration in the sink/source fluid (ML^{-3}), λ is the decay rate (T^{-1}), R_f is the retardation factor (dimensionless), t is time (T), and x_i are Cartesian coordinates (L).

The second term in equation 1 represents solute transport by advection. The consideration of advective solute flux is straightforward if the HFB Package is active. Ground-water-flow velocities can be computed directly from the computed heads

and specified porosity. Because the HFB Package assumes zero storage capacity within the barrier and negligible barrier width, however, the time of transport across cells that border a barrier may not be highly accurate. The magnitude of this error likely will be proportional to the difference between the cell width and the barrier width. If this source of error is (or is likely to be) relatively large, then the HFB Package should not be used in a solute-transport simulation.

The third term in equation 1 represents solute transport by hydrodynamic dispersion. This conventional Fickian model assumes that the driving force is the concentration gradient and that the dispersive flux occurs from higher concentrations towards lower concentrations. The coefficient of hydrodynamic dispersion (D_{ij}) may be related to the velocity of ground-water flow, and for an isotropic aquifer the dispersivity tensor can be defined in terms of the longitudinal and transverse dispersivities, α_L and α_T, as

$$D_{ij} = (\alpha_L - \alpha_T)\frac{V_i V_j}{|V|} + (D_m + \alpha_T |V|)\delta_{ij}, \quad (2)$$

where V_i and V_j are components of the velocity vector in the i and j directions, respectively; $|V|$ is the magnitude of velocity; D_m is the effective coefficient of molecular diffusion $(L^2 T^{-1})$; $\delta_{ij} = 1$ if $i = j$ and $\delta_{ij} = 0$ if $i \neq j$ (see Konikow and others, 1996).

The GWT Process numerically solves the transport equation using operator splitting techniques in which the advective terms are solved separately from the terms representing dispersive fluxes. One approach uses the method of characteristics, as described by Konikow and others (1996) and by Kipp and others (1998). Another approach uses a finite-volume Eulerian-Lagrangian localized adjoint method (Heberton and others, 2000). In all cases, the transport solver uses the ground-water fluxes computed by *MODFLOW* to calculate the flow velocity, which controls both advective and dispersive solute fluxes.

All components of the dispersion tensor must be considered in solving equations 1 and 2. The complexity of this expansion is illustrated by applying explicit (forward-in-time) finite-difference approximations to the component of the dispersive flux in the x-direction across the cell face at $(j + 1/2, i, k)$. For example, the approximation may be written as

$$-\left(\varepsilon b D_{xm}\frac{\partial C}{\partial m}\right)_{j+1/2,i,k} = -\left(\varepsilon b D_{xx}\right)_{j+1/2,i,k}\frac{\left(C_{j+1,i,k} - C_{j,i,k}\right)}{\Delta x}$$

$$-\left(\varepsilon b D_{xy}\right)_{j+1/2,i,k}\frac{\left(C_{j,i+1,k} + C_{j+1,i+1,k} - C_{j,i-1,k} - C_{j+1,i-1,k}\right)}{4\Delta y}$$

$$-\left(\varepsilon b D_{xz}\right)_{j+1/2,i,k}0.5\left(\frac{C_{j+1,i,k+1} - C_{j+1,i,k-1}}{2B_{j+1,i,k}} + \frac{C_{j,i,k+1} - C_{j,i,k-1}}{2B_{j,i,k}}\right), \quad (3)$$

where m is a summation index ranging from 1 to 3, so that m would correspond, in turn, with x, y, and z; b is the saturated thickness of a cell, and $2B_{j,i,k} \equiv b_{j,i,k} + 1/2\,(b_{j,i,k-1} + b_{j,i,k+1})$ is the vertical distance between nodes $(j,i,k+1)$ and $(j,i,k-1)$. For simplicity, equation 3 assumes that both Δx and Δy are constant. The three terms on the right side of equation 3 describe the dispersive flux of solute in the x-direction (across the cell face at $j+1/2$) because of concentration gradients in the x-, y-, and z-directions, respectively.

A representative part of a grid is illustrated in figure 1 that shows which nodes are used to estimate concentration gradients for the D_{xx} and D_{xy} terms in equation 3. The concentration gradient in the x-direction at the cell face located at the $j+1/2$ location is associated with the first term (D_{xx}) and is
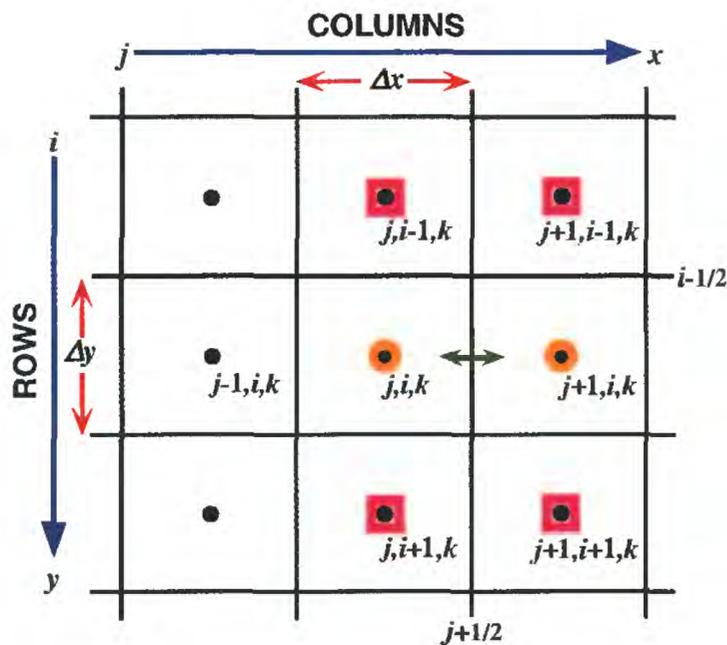
COLUMNS

EXPLANATION

- Node of finite-difference cell
- Reference cell face for dispersive flux
- Nodes used for D_{xx} term
- Nodes used for D_{xy} term

Figure 1. Representative part of one layer of a three-dimensional, block-centered, finite-difference grid showing cells that are used to calculate concentration gradients in x- and y-directions for the solute-transport model, *MODFLOW-GWT*.

estimated directly from the difference in concentration at the adjacent nodes ($j+1,i,k$ and j,i,k) divided by the distance between them (Δx). The second and third terms are more problematic as they include the cross-product (or off-diagonal) terms of the dispersion tensor. A lower order of accuracy is associated with the estimation of the corresponding concentration gradient because the concentration gradient in the y-direction cannot be computed directly at the $j+1/2$ location. Instead, for the D_{xy} term, a common approximation for $\partial C/\partial y$ at $j+1/2$ involves averaging the estimates of $\Delta C/\Delta y$ at the two adjacent nodes ($j+1,i,k$ and j,i,k), both of which must be calculated over distances of twice the grid spacing. For example, $\Delta C/\Delta y$ at $j+1,i,k$ equals $C_{j+1,i+1,k} - C_{j+1,i-1,k}/2\Delta y$.

These finite-difference approximations work well if the concentration field varies smoothly over the area of a few grid cells. They are consistent with an assumption that concentrations vary linearly between adjacent nodes of the grid. Where an artificial barrier wall has been constructed, however, it is often to contain contaminated ground water. In such areas, the assumption about locally smooth concentration changes over the area of three grid cells may not be appropriate because the wall is designed to provide a barrier to solute migration. Thus, concentrations and concentration gradients may change drastically across the narrow zone that coincides with the barrier wall. As a result, concentration differences across the barrier wall may not be indicative of local concentration gradients on just one side of the barrier.

The implication of these spatial concentration differences for the numerical methods is illustrated by an example shown in figure 2, which shows a horizontal-flow barrier coinciding with $i-1/2$ (that is, aligned with the cell faces between row i and row $i-1$ in the grid). In this example, the barrier separates an area where the ground water has relatively
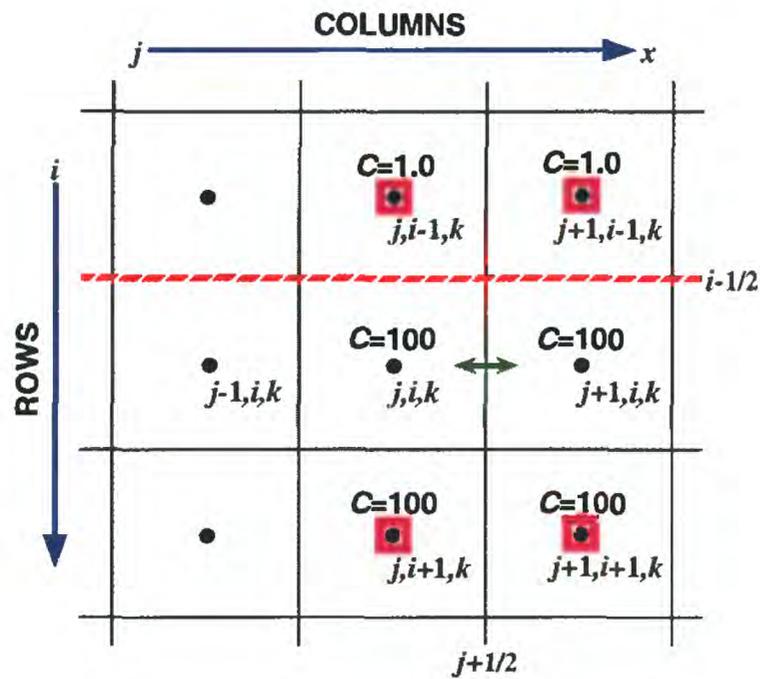
COLUMNS

EXPLANATION

- Node of finite-difference cell
- Reference cell face for dispersive flux
- Nodes used for D_{xy} term

$C=100$ Average concentration in finite-difference cell

Horizontal-flow barrier

Figure 2. Hypothetical concentrations at cells used to calculate dispersive flux in the x-direction because of the concentration gradient in the y-direction for the horizontal-flow barrier example case.

high concentrations ($C = 100.0$) in rows i and $i+1$ from an area having low concentrations ($C = 1.0$) in row $i-1$. There should be no dispersive flux in the x-direction across the cell face at $j+1/2,i$ driven by the

concentration gradient in the x-direction because the concentration gradient at $j+1/2,i$ is zero. In addition, within the "contaminated" zone south of the barrier, the concentrations are uniform and the gradient in the y-direction also is zero. Across the cell face at $j+1/2,i$, there also should be no dispersive flux in the x-direction caused by a concentration gradient in the y-direction. If the standard finite-difference approximation for the cross-product terms is applied (equation 3), however, a nonzero concentration gradient will be computed in the y-direction at $j+1/2,i$ as $\partial C/\partial y \approx (100\text{-}1)/2\Delta y = 49.5/\Delta y$. Assuming that the velocities are nonzero, this nonzero concentration gradient will cause a solute flux to be computed erroneously across the cell face at $j+1/2,i$.

A reasonable solution to the numerical problem described above can be derived by assuming that, in the presence of a barrier wall, the concentration gradient immediately adjacent to one side of the barrier should be estimated only on the basis of differences in nodal concentrations on the same side of the barrier. For example, in the case illustrated in figure 2, $(\partial C/\partial y)_{j,i,k} \approx (C_{j,i+1,k} - C_{j,i,k})/\Delta y$, which is equivalent to assuming that $(\partial C/\partial y)_{j,i,k} \approx (\partial C/\partial y)_{j,i+1/2,k}$. Modifying equation 3 for this approximation allows the term for the dispersive flux in the x-direction due to a concentration gradient in the y-direction to be given as

$$-\left(\varepsilon b D_{xy} \frac{\partial C}{\partial y}\right)_{j+1/2,i,k} = -\left(\varepsilon b D_{xy}\right)_{j+1/2,i,k} \frac{\left(C_{j,i+1,k} + C_{j+1,i+1,k} - C_{j,i,k} - C_{j+1,i,k}\right)}{2\Delta y} . \quad (4)$$

The assumption represented by equation 4 for the D_{xy} term of the dispersion tensor, and an analogous expression for the D_{yx} term, is illustrated in figure 3. This modification has been incorporated into a revised version of the *MODFLOW-GWT* model. In this new code, a check is performed to determine if a cell is adjacent to a horizontal-flow barrier. If it is, then the horizontal concentration gradients used to calculate the cross-product dispersive flux of solute in the horizontal plane are estimated using modified finite-difference formulations, as in equation 4.

Just as barrier walls have hydraulic properties different from those of an aquifer, the dispersive characteristics of barriers also may differ from those of an adjacent aquifer. For example, because constructed barriers typically have relatively homogeneous material properties, their dispersivity values probably would be smaller than those of an adjacent heterogeneous aquifer. Therefore, the *MODFLOW-GWT* model was modified to allow the user to assign unique dispersivity and diffusion coefficient values for the properties of a horizontal-flow barrier represented by HFB. These values are assumed to be effective for solute transport across the cell faces that correspond to the locations of the HFB barriers. Hence, these specified values of α_T, α_L, and D_m are used in equation 2 when calculating the dispersion coefficients for model cells adjacent to HFB barriers. Assigning a lower value for either the effective dispersivity or diffusion coefficients or both for the barrier than for
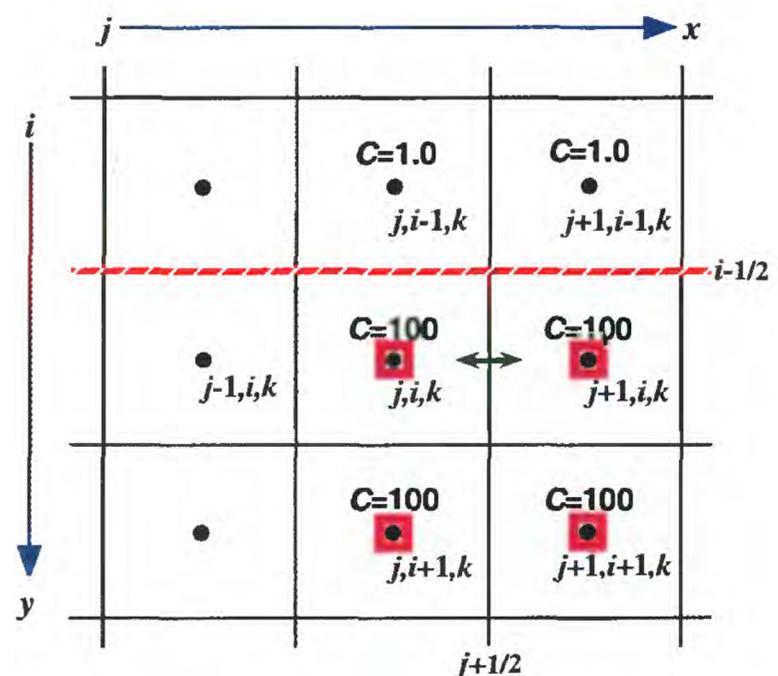
EXPLANATION

- **•**   Node of finite-difference cell
- **↔**   Reference cell face for dispersive flux
- **▣**   Nodes used for D_{xy} term
- *C*=100   Average concentration in finite-difference cell
- **----**   Horizontal-flow barrier

Figure 3. Cells used to calculate the dispersive solute flux for the D_{xy} term using the CHFB package of *MODFLOW-GWT* (same hypothetical case as shown in figure 2).

the aquifer can compensate for the fact that the width of a barrier is not specified explicitly but rather is represented implicitly by a lower inter-cell conductance value. Thus, the rate of diffusive and dispersive transport through the implicitly represented barrier can be reduced to yield a better approximation of the effects of slow transport through the barrier material.

COMPUTER PROGRAM

The modifications to the *MODFLOW-GWT* code described in this report are compatible with *MODFLOW-2000* (Harbaugh and others, 2000). The GWT process is described by Konikow and others (1996), Kipp and others (1998), and Heberton and others (2000). Two major modifications were made to the *MODFLOW-GWT* code: (1) specification of different dispersive properties for HFB barriers than for the aquifer, and (2) cross-dispersive solute flux calculations use alternate cells to determine concentration gradients depending on location of HFB faces. These modifications only are available if the

HFB package and the GWT Process are activated. The resulting new package for computing Concentration with HFB is called the CHFB package. The computer coding is written in standard FORTRAN-77 and FORTRAN-90, and it has been successfully compiled and executed on multiple platforms, including Pentium-based personal computers Unix workstations. The names and functions of subroutines added to the GWT Process are listed in table 1.

The new package is implemented by including the CHFB File Type in the GWT name file. Input data requirements for the CHFB package are described in appendix A. Selected input and output files are included in appendices B and C, respectively.

Table 1. *MODFLOW-GWT* subroutines for CHFB package

Subroutine	Description
GWT1HFB6RP	Read separate dispersivity and diffusion parameters for barriers defined using the HFB (Horizontal-Flow Barrier) package
DSP6HFB	Update array of dispersion coefficients using specified barrier properties.
DSP6APH	Explicitly calculate change in concentration due to dispersion; use alternate cells for determining concentration gradient with respect to location of HFB barriers.
CR5DSPH	Implicitly calculate change in concentration due to dispersion; use alternate cells for determining concentration gradient with respect to location of HFB barriers.
ELLDISH	Build dispersion integral; use alternate cells while filling integral array with respect to location of HFB barriers.

NUMERICAL EXPERIMENTS

A test problem was designed that is similar (but not identical) to the problem used by Neville and others (1998). The test problem described here conceptualizes a thin permeable aquifer in which a rectangular zone of contaminated ground water is encapsulated by a low-permeability wall that is 5 ft wide and extends from the land surface to the base of the aquifer, which overlies impermeable material. The finite-difference grid for this test problem is shown in figure 4. Values of physical parameters describing the problem are summarized in table 2. The area within the barrier is capped (no recharge) and contains an initial concentration (C_0) of 100.0 (C_0 = 0.0 elsewhere). (Note that the problem is set up in terms of relative concentrations, which are dimensionless.) The aquifer is 25 ft thick with uniform properties. The hydraulic conductivity of the barrier is 10^{-4} times that of the aquifer. The flow system is at steady state and is controlled by a constant-head boundary condition (at $h = 20.0$ ft) in the far right column of cells of the grid, no-flow boundaries elsewhere,
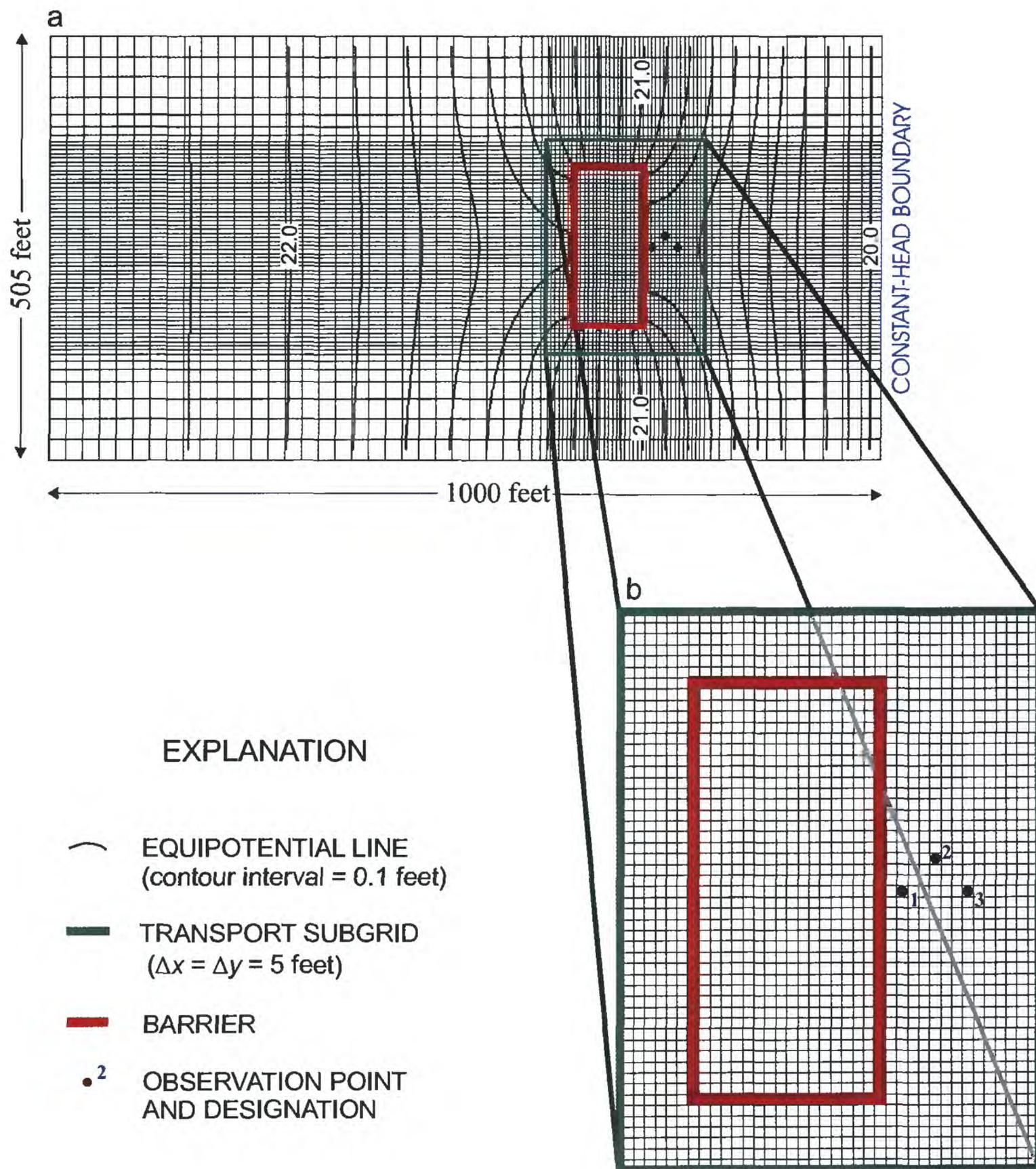
Figure 4. Grid design for test problem using *MODFLOW-GWT*, showing (a) primary variably spaced *MODFLOW* grid and calculated steady-state heads, and (b) uniformly spaced transport subgrid. Far right column of cells of primary grid represents a constant-head boundary condition (*h* = 20 feet).

Table 2. Physical parameters for test problem

[ft/d, feet per day; ft^2/d, feet squared per day]

Parameter	Aquifer	Barrier
K_h	28.25 ft/d	0.002835 ft/d
ε	.3	.3
b	25.0 ft	25.0 ft
α_L	5.0 ft	5.0 or 0.5 ft*
α_{TH}	.25 ft	.25 or 0.025 ft*
α_{TV}	.0	.0
D_m	10^{-4} ft^2/d	10^{-4} ft^2/d or 10^{-5} ft^2/d*
R_f	1.0	1.0
Recharge	2.2815×10^{-3} ft/d	.0
C_0	.0	100.0
$C_{Recharge}$	.0	.0

* Reduced values of dispersivity and diffusion coefficients were used for some simulations

and by a uniform recharge rate of 2.2815×10^{-3} ft/d over the uncapped aquifer. The contaminant is assumed to be nonreactive. A stress period of 5,000 days was simulated. The calculated steady-state head distribution for this problem is shown in figure 4a. The heads indicate that regional flow is from left to right and that most flow is diverted around the barrier.

For efficiency, the transport equation was solved in a subgrid of the area having the finest discretization, where the grid cells are spaced uniformly at 5 ft by 5 ft (see fig. 4b). Three cells downgradient from the barrier were designated as observation points (locations shown in fig. 4), where concentration data were recorded at every transport time increment in the simulation to capture and evaluate the breakthrough profile. In each simulation, the transport equation was solved using the method of characteristics with an implicit solution of the dispersion terms (Kipp and others, 1998). Values for numerical parameters are summarized in table 3 (see Konikow and

others, 1996, and Kipp and others, 1998, for detailed descriptions of numerical methods and parameters). A custom initial particle distribution was used to capture the details of advective transport. Each cell contained an initial distribution of 347 particles at the beginning of the simulations. Note that this distribution is a much greater density of particles than normally used (the maximum default initial particle distribution is 27 particles per cell). It was found from initial numerical solutions that, because of the heterogeneity and curvilinear flow field induced by the contrast in hydraulic conductivity between the barrier and the aquifer, use of fewer than 347 particles could not yield an adequate representation of concentration changes caused by advective transport. The custom placement used three rows of 99 particles (aligned with the main flow direction) and five columns of 10 particles each. This distribution resulted in reasonably accurate solute mass balances, although some numerical oscillations remained.

Table 3. Numerical specifications for test problem

Parameter	Value or Setting
Transport Ftype	MOCIMP
Primary MODFLOW Grid	
Layers	1
Rows	65 or 29*
Columns	80 or 53*
Transport Subgrid	
Layers	1
Rows	51 or 17*
Columns	38 or 13*
NPTPND	347 or 696*
CELDIS	1.0
FZERO	1×10^{-4} or 1.5×10^{-4}*
INTRPL	1
FDTMTH	1.0
NCXIT	2
IDIREC	1
EPSSLV	1×10^{-5}
MAXIT	100
CINFL	.0
NUMOBS	3

* Values used for coarse-grid simulation

A sequence of simulations was used to evaluate the results and compare alternative solution methods. In the first simulation case, the barrier is represented explicitly by defining a rectangular strip of cells (see figs. 4 and 5a) having a hydraulic conductivity lower than the surrounding cells. In this case, the cell dimensions capture the exact dimensions of the barrier. In the subsequent simulations the barrier wall is represented implicitly by using the HFB package to define the conductance properties of the outside faces of the original barrier cells. A schematic of the grid for the implicit representation of the barrier is shown in figure 5b, which can be compared to the grid for the explicit representation shown in figure 5a. The hydraulic properties of the barrier are represented on the cell faces aligned with the

outer edge of the actual barrier location so that the head and velocity distributions relative to the locations of the observation points would be as similar as possible between the two sets of conditions, which would allow for a more meaningful comparison. However, this conceptualization causes the area enclosed by the implicit barrier to be slightly larger than the equivalent area of aquifer enclosed by the explicit barrier. Therefore, the observation points in the implicit simulations are 5 ft closer to cells with a high initial concentration than the equivalent observation points in the explicit simulations.

A concentration map of the transport subgrid for the simulation in which the barrier is defined explicitly (fig. 6a) shows that a thin plume of low concentration has migrated through the downgradient side of the barrier

EXPLANATION

— FINE GRID
($\Delta x = \Delta y = 5$ feet)

— COARSE GRID
($\Delta x = \Delta y = 15$ feet)

▬ BARRIER (WIDTH = 5 feet)

| IMPLICIT BARRIER LOCATION

• OBSERVATION POINT
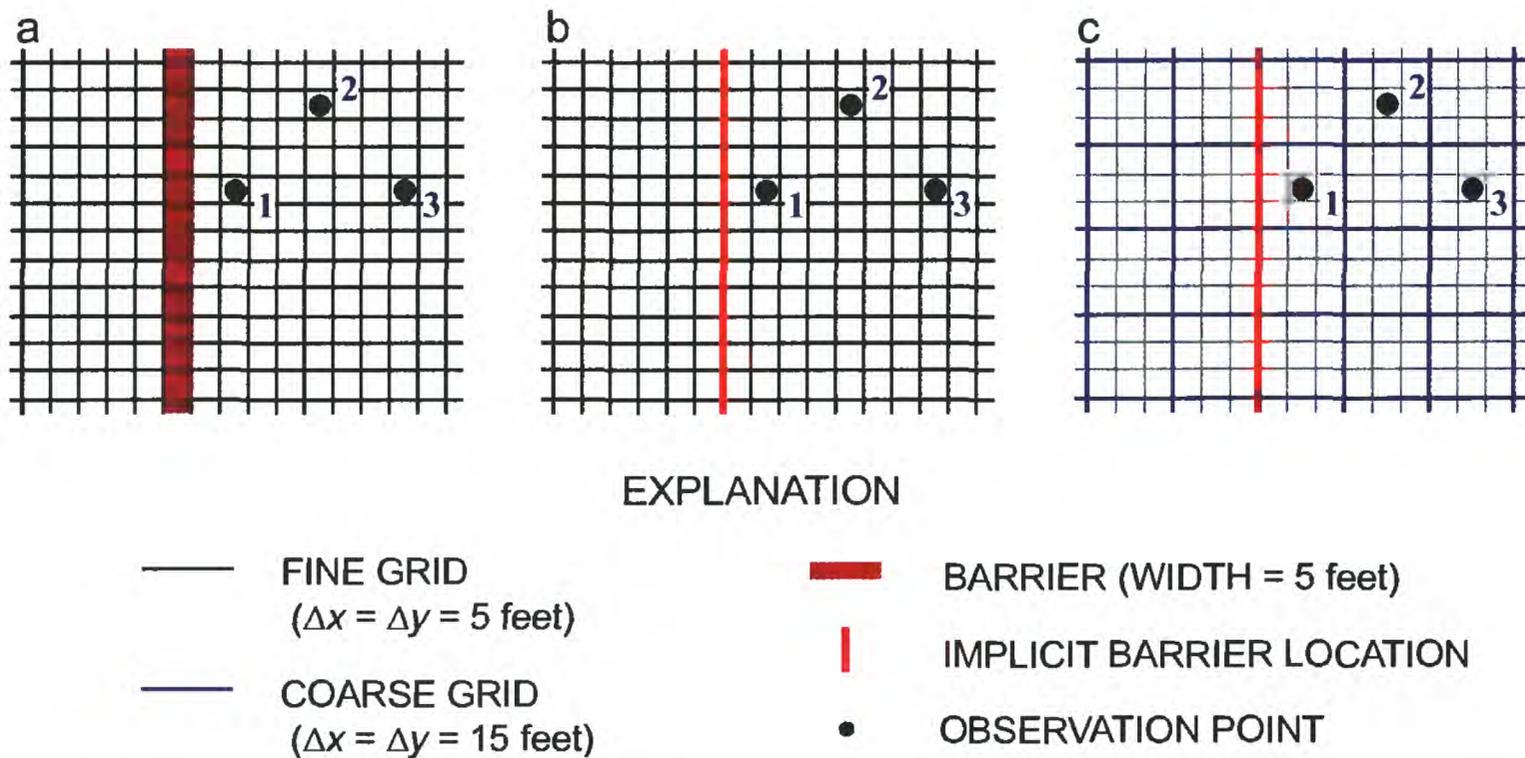
Figure 5. Selected part of transport subgrid illustrating grid modifications for numerical experiments using *MODFLOW-GWT*: (a) explicit representation of barrier, (b) implicit representation of barrier, and (c) implicit barrier using coarse grid.

(from left to right). Analysis of changes in the spatial distributions of solute at various times indicates that the solute that escapes from the barrier wall does so by both dispersive transport through the barrier and by advective transport. There is a very small amount of upstream dispersion on the left side of the barrier (near row 25, column 5). Solute breakthrough curves at each observation cell are shown as solid lines in figure 7. These results for the explicit simulation show that the concentration gradually increases over time to a maximum value of about 19.0 at observation point 1, nearest to the barrier wall. The small oscillations in the breakthrough curves are an artifact of the particle-tracking routine, and do not affect the overall accuracy or interpretation of the results.

To provide a basis of comparison, the first of the simulations in which the barrier is represented implicitly was run using the unmodified *MODFLOW-GWT*

model. The HFB package is used to represent the barrier implicitly (by defining lower inter-cell conductance values—the width of the barrier is not modeled explicitly). The map of concentration from this simulation (fig. 6b) shows that although the overall shape of the plume is maintained, higher solute concentrations are calculated near the barrier wall and the downgradient plume is larger. That is, if it is assumed that the numerical solution for the explicit barrier is accurate, then simulating the barrier with HFB allows too much solute to cross the barrier, which is consistent with the findings of Neville and others (1998). The concentrations at the observation points for this implicit representation (dashed lines in fig. 7) rapidly increase (to a maximum of about 39.0 for observation point 1) and then gradually decline. The concentrations calculated for the implicit case are too high, especially at early times in the simulation. The late gradual decline in concentration
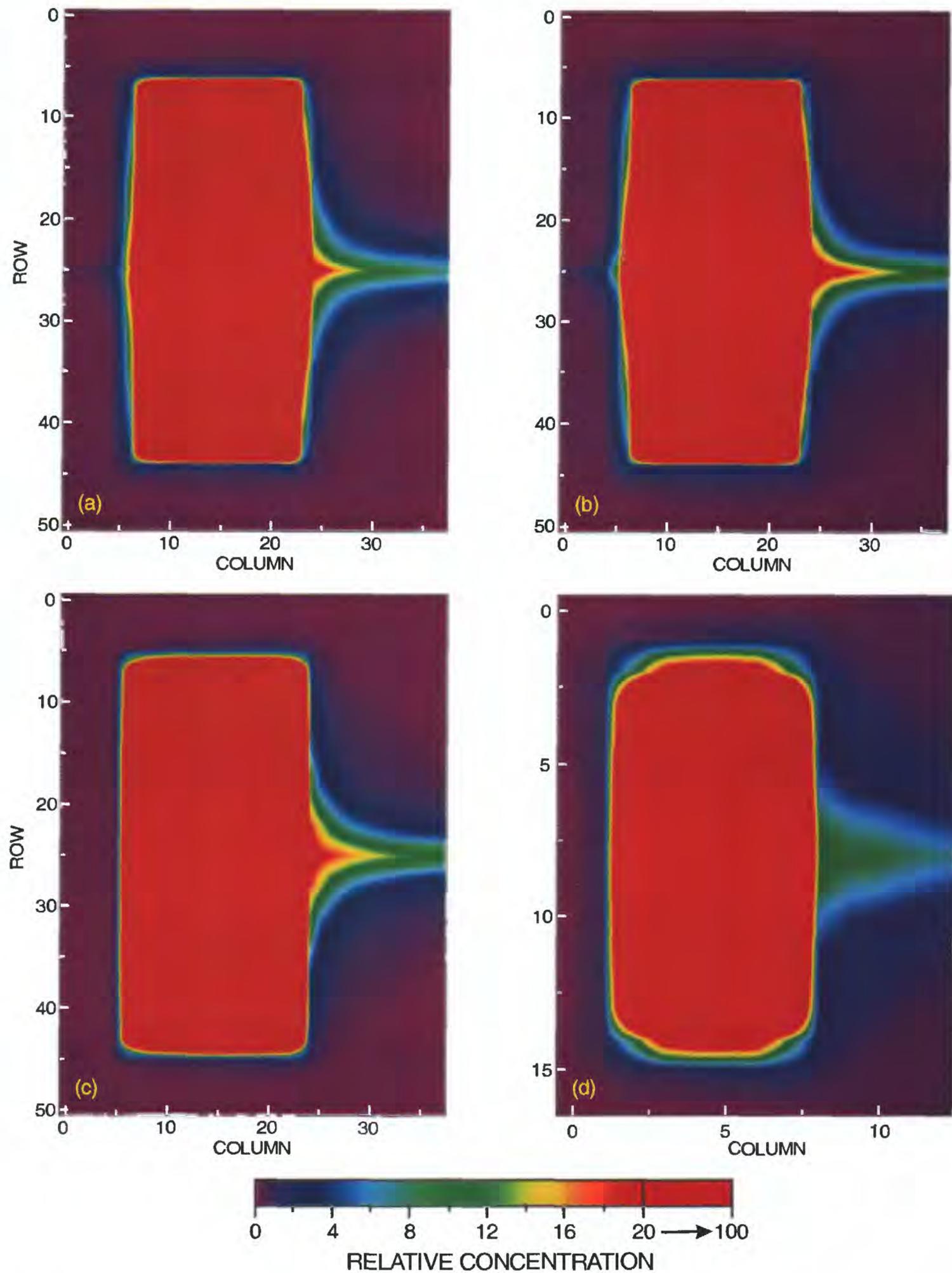
Figure 6. Concentration maps of test problem results at 5,000 days for (a) explicit representation of barrier, (b) implicit representation of barrier using unmodified GWT code, (c) implicit representation of barrier using CHFB package for transport (barrier dispersivities and diffusion coefficients set to one-tenth of the respective aquifer properties), and (d) implicit representation using CHFB on a coarse grid. Areas with concentration from 20.0 to 100.0 are colored red.
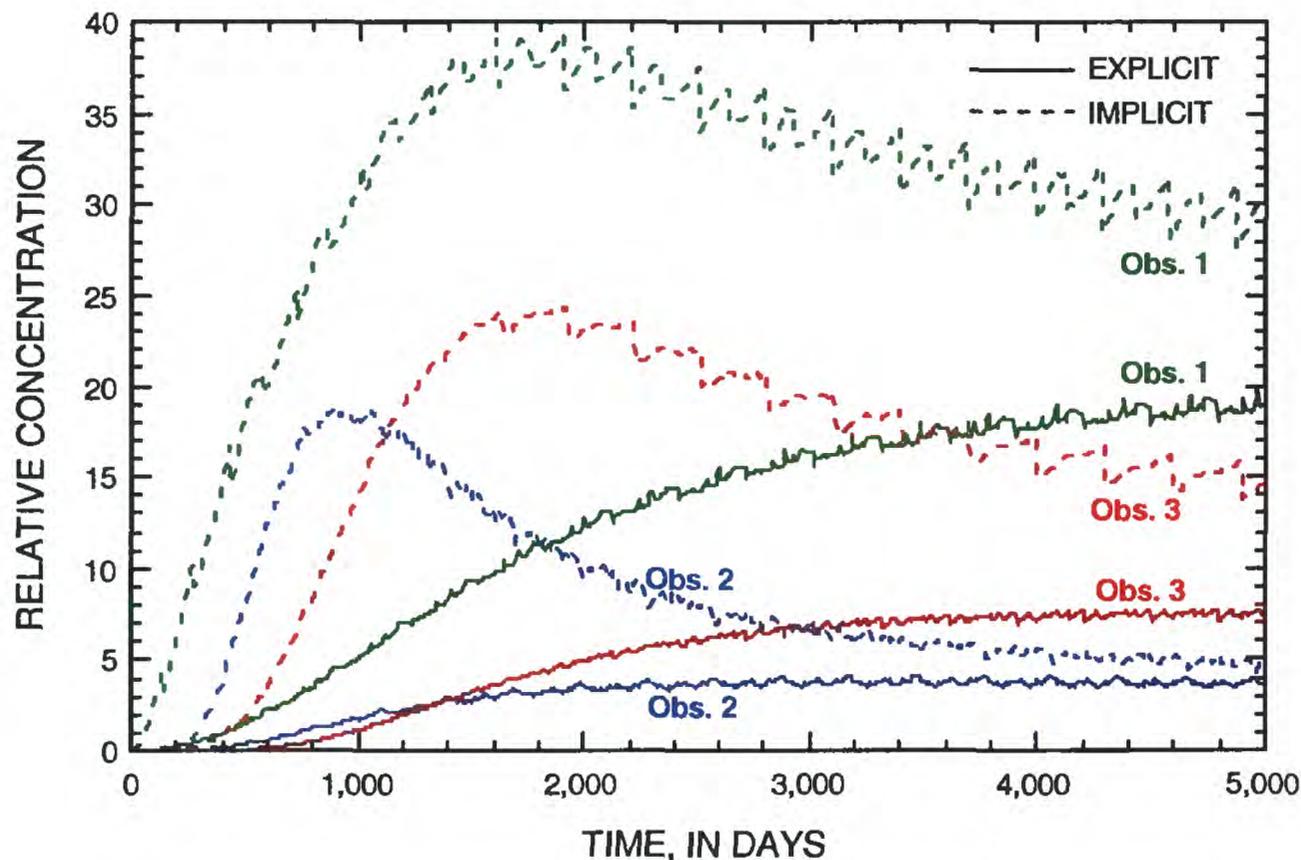
Figure 7. Breakthrough curves at three observation points for explicit (solid lines) and implicit (dashed lines) representations of barrier using unmodified *MODFLOW-GWT* code. Locations of observation points are shown in figure 4.

reflects the slower dispersive transfer because of lower concentration gradients at later times between the contained area and the active flow domain of the simulated aquifer.

In the next set of simulations, the effects of the new CHFB package were evaluated. First, the CHFB package was activated while keeping all parameter values the same (see table 2). The effect is illustrated by a comparison of breakthrough curves for observation point 1 (see fig. 8). The results for this simulation (curve c) show *reduced concentrations relative to* curve b for the unmodified code, and are closer to the results for the explicit case (curve a). However, the calculated concentrations are still too high relative to the explicit solution, especially at early times and immediately downgradient from the barrier. To assess the relative contributions of advection and dispersion to the difference, the CHFB simulation was rerun reducing the dispersive properties of

the barrier to one-tenth of those in the aquifer and to zero. The results of activating the CHFB package and setting the dispersive properties of the barrier equal to one-tenth of those in the aquifer are illustrated in figure 6c and by curve d in figure 8 (further reducing the dispersive properties of the barrier to zero values had no appreciable additional effect on the results). The magnitude of the effect of reducing the dispersivity and diffusion coefficients of the barrier can be evaluated by comparing the breakthrough curves at observation point 1 for the simulation using barrier dispersivities equal to one-tenth of those in the aquifer (curve d in fig. 8) to the simulation using barrier dispersivities equal to those in the aquifer (curve c in fig. 8). The difference between curve c and curve d is due solely to the difference in the values of the dispersivity and diffusion coefficients specified for the barrier. The difference is largest at early times and the two curves converge towards the end of the simulation
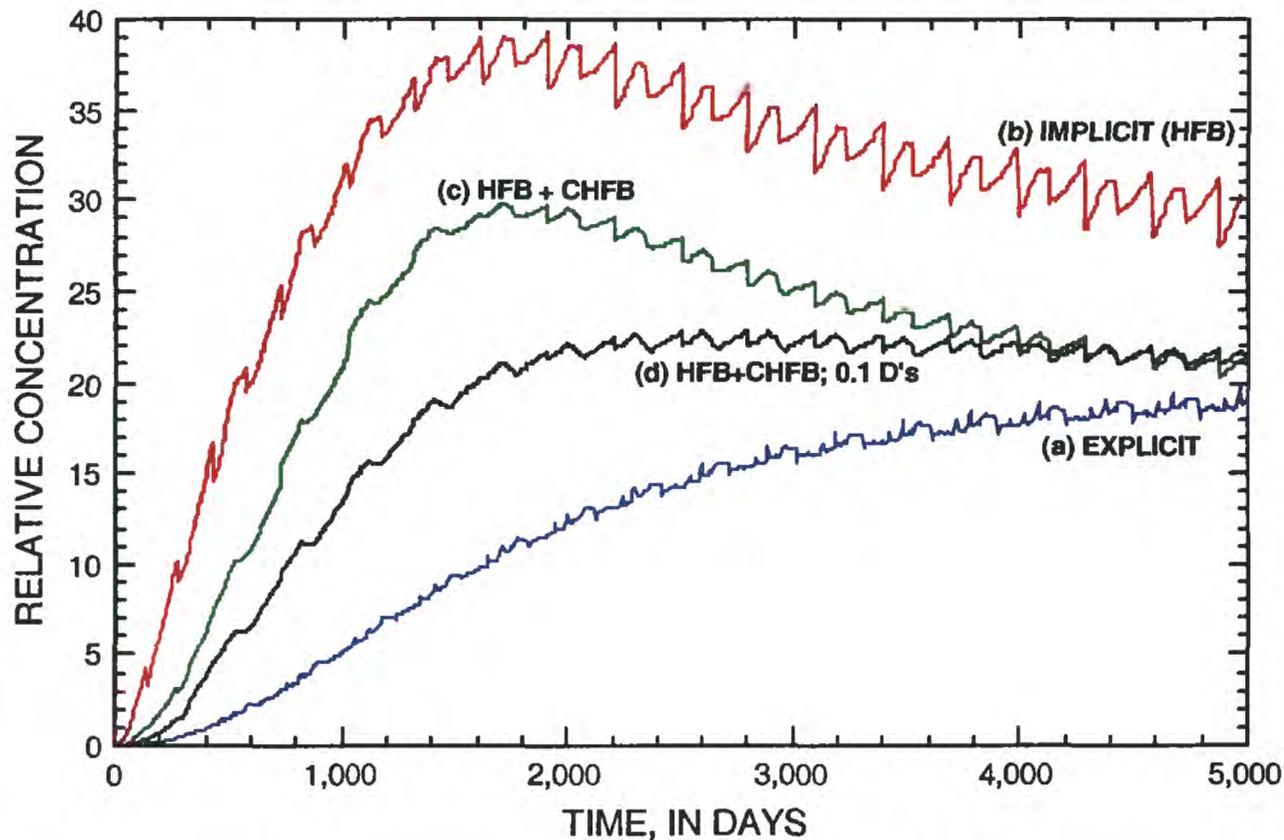
Figure 8. Breakthrough curves at observation point 1 for (a) explicit representation of the barrier, (b) implicit representation of barrier using unmodified *MODFLOW-GWT* code, (c) implicit representation of barrier using CHFB package for transport (barrier dispersivities and diffusivity set to one-tenth of the respective aquifer properties), and (d) implicit representation of barrier using CHFB package for transport (barrier dispersivities and diffusivity set equal the respective aquifer properties).

period. Comparison of the concentration map at the end of the simulation period (fig. 6c) with those for the explicit representation of the barrier (fig. 6a) shows that solute transport through the barrier still is slightly overestimated when CHFB is active. This overestimation mainly is caused by errors in estimating advective transport across the HFB barrier, which arise from the assumption of zero storage capacity within the barrier and negligible barrier width; the CHFB package is not designed to control this type of error. However, comparison of the CHFB results with those using the unmodified code for the implicit representation (fig. 6b and curve b in fig. 8) shows that CHFB yields a large improvement by reducing the amount of solute transported across the barrier due to dispersion and diffusion. At early times, this reduction in dispersive and diffusive flux

across the barrier is related partly to the reduced magnitude of the dispersivity and diffusion coefficients specified for the barrier in the simulation represented by curve d in figure 8, but after early transient effects are passed, the reduction is related primarily to the improved method to calculate concentration gradients more accurately near a barrier. The effect of the improved calculation method can be seen most clearly on the upstream side of the barrier, where upstream dispersion across the barrier is eliminated (fig. 6c).

Overall, the modified code more accurately simulates the breakthrough than the unmodified code (fig. 8). Both of the CHFB simulations yielded results closer to the explicit representation (curve a) than did the implicit representation with the unmodified code (curve b). The residual difference between curves a and d can be

Numerical Experiments 15

attributed primarily to the advective transport error. The difference between curves b and c is a direct measure of the improvement gained from the new method for calculating dispersive solute flux across an implicitly represented barrier. Relative to the implicit representation using the unmodified code, the CHFB results show an improvement in the estimation of the peak concentration and a much closer match to the final concentration of the explicit case.

Because the advantage of using the HFB package is to provide computational efficiency by enabling a relatively narrow feature to be represented while using a coarse grid, the final evaluation used the CHFB package for a simulation with a coarser grid. In this case the grid dimensions within the transport subgrid were increased by a factor of three in both the row and column directions, so that $\Delta x = \Delta y = 15$ ft. One reason for selecting this ratio is that the spatial locations for the observation points are exactly the same for both grids, which allows a direct comparison of breakthrough curves. As illustrated in figure 5c, the observation points are located exactly at the centers of the cells of the coarse grid and at the same distances downgradient from the implicit barrier as for the fine grid case (fig. 5b).

For the coarse grid case, the dispersive and diffusive properties of the barrier were set equal to those of the aquifer. Also, the number of particles distributed to each cell was increased to 696 (three rows of 199 particles and one column of 99 particles) to help offset the loss of resolution induced by coarsening the grid. The solution for the coarse grid was reached much more efficiently than with the finer grid. The relative computational times for various test cases indicates that the running time for the coarse-grid implicit representation was reduced to only about 6 percent of that for the explicit simulation (table 4). The concentration map depicting the results for this simulation (fig. 6d) shows that peak concentrations downgradient of the barrier are lower with the coarse grid, but the solute is spread out over a larger area. This result is expected because of coarsening the grid in the presence of a relatively narrow plume. The concentration breakthroughs for this case

Table 4. Computational times for selected simulations using *MODFLOW-GWT*
[CPU, Central Processing Unit; s, seconds]

Barrier representation	Number of finite difference cells in solute-transport subgrid	Number of transport time increments	CPU time (s)*
Explicit	1938	828	1512
Implicit (HFB only)	1938	828	1518
Implicit (HFB and CHFB)	1938	828	1392
Implicit (HFB and CHFB; coarse grid)	221	204	96

* All simulations were run on a Pentium 4 PC running Windows 2000 with 768 MB RAM and a 1.5 GHz processor. Compaq Visual Fortran version 6.5 was used to compile *MODFLOW-GWT*.

are compared to the explicit simulation in figure 9. By the end of the simulation period, the smearing effect causes concentrations with the coarse grid to be too low near the barrier (observation point 1) and too high farther downgradient from the barrier (observation points 2 and

3). However, the overall solute spreading pattern is similar. The user must be aware that use of a coarser grid can have a greater effect on the solute-transport solution than on the calculated heads, and must decide whether the gain in efficiency is worth the potential loss of precision.
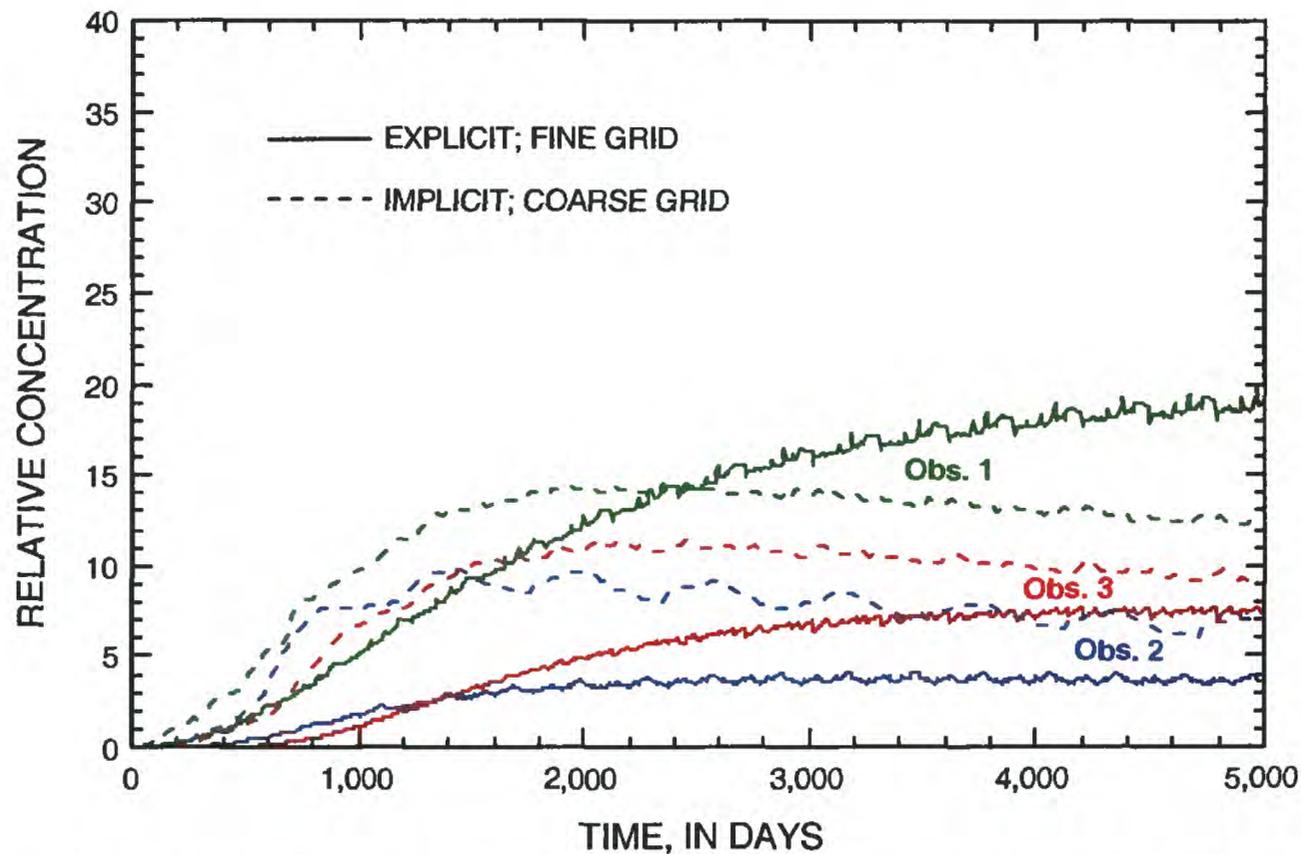
Figure 9. Breakthrough curves at three observation points for explicit (solid lines) and coarse-grid implicit (dashed lines) representations of barrier using *MODFLOW-GWT*. Locations of observation points are shown in figure 4.

SUMMARY AND CONCLUSIONS

Explicit simulation of horizontal, low-permeability barrier walls can be effective, but may be inefficient. Efficiency is gained if the hydraulic properties of the barrier can be represented implicitly, such as through application of the HFB package of *MODFLOW*. If solute transport is simulated simultaneously with flow, then the conventional transport model likely will over-estimate the dispersive solute flux through an implicitly represented barrier. The new CHFB Package in the modified *MODFLOW-GWT* solute-transport model

developed by the USGS (1) allows the specification of different dispersive properties for HFB barriers than for the aquifer, and (2) calculates dispersive fluxes to reflect that concentration differences across a barrier may not provide an accurate estimate of the local concentration gradients on each side of the barrier. The ability to specify unique dispersivity values for a barrier allows for greater flexibility in simulating field conditions and in the effort to calibrate to observed concentrations. The CHFB Package is compatible with the

published HFB package, but requires an additional input data file to specify barrier transport properties (described in appendix A). Activation of the CHFB Package provides a more accurate solution to the solute-transport equation when implicitly representing a horizontal-flow barrier in a *MODFLOW* simulation.

REFERENCES

Harbaugh, A.W., and McDonald, M.G., 1996, User's documentation for MODFLOW-96, an update to the U.S. Geological Survey modular finite-difference ground-water flow model: U.S. Geological Survey Open-File Report 96-485, 56 p.

Harbaugh, A.W., Banta, E.R., Hill, M.C., and McDonald, M.G., 2000, MODFLOW-2000, The U.S. Geological Survey modular ground-water model—User guide to modularization concepts and the ground-water flow process: U.S. Geological Survey Open-File Report 00-92, 121 p.

Heberton, C.I., Russell, T.F., Konikow, L.F., and Hornberger, G.Z., 2000, A three-dimensional finite-volume Eulerian-Lagrangian Localized Adjoint Method (ELLAM) for solute-transport modeling: U.S. Geological Survey Water-Resources Investigations Report 00-4087, 63 p.

Hsieh, P.A., and Freckleton, J.R., 1993, Documentation of a computer program to simulate horizontal-flow barriers using the U.S. Geological Survey's modular three-dimensional finite-difference ground-water flow model: U.S. Geological Survey Open-File Report 92-477, 32 p.

Kipp, K.L., Jr., Konikow, L.F., and Hornberger, G.Z., 1998, An implicit dispersive transport algorithm for the U.S. Geological Survey MOC3D solute-transport model: U.S. Geological Survey Water-Resources Investigations Report 98-4234, 54 p.

Konikow, L.F., Goode, D.J., and Hornberger, G.Z., 1996, A three-dimensional method of characteristics solute-transport model (MOC3D): U.S. Geological Survey Water-Resources Investigations Report 96-4267, 87 p.

McDonald, M.G., and Harbaugh, A.W., 1988, A modular three-dimensional finite-difference ground-water flow model: U.S. Geological Survey Techniques of Water-Resources Investigations, book 6, chap. A1, 586 p.

Neville, C.J., Riley, M.J., and Zheng, C., 1998, Implicit modeling of low permeability features: an appraisal for solute transport, *in* Poeter, Eileen, Zheng, Chunmiao, and Hill, Mary, eds., MODFLOW 98 Proceedings: Colorado School of Mines, Golden, Colorado, 1998, v. 1, p. 353-362.

APPENDIXES

Note: References cited in the appendixes are listed in the References section of the report

APPENDIX A: DATA INPUT INSTRUCTIONS FOR CHFB PACKAGE

The GWT name file consists of records defining the names and unit numbers of the files. Each "record" consists of a separate line of data. Following is a description of the new optional file type that can be included in the transport name file to activate the CHFB package.

1. Data: FTYPE   NUNIT   FNAME

FTYPE   The file type:

    CHFB   Transport properties for Horizontal Flow Barriers and alternate calculation of dispersive flux near HFB cells *[optional]*. This option only should be used if the HFB package is active.

NUNIT   The FORTRAN unit number used to read from and write to files. Any legal unit number other than 97, 98, and 99 (which are reserved by *MODFLOW*) can be used provided that it is not previously specified in the *MODFLOW* name file.

FNAME   The name of the file.

CHFB Input File

Activating the CHFB package requires the user to specify effective dispersivities and diffusion coefficients for solute transport across cell faces corresponding to each of the barriers defined using the Horizontal Flow Barrier (HFB) package. Data are specified for sequential groups of barriers with identical properties (where a "group" can include as few as one barrier or as many as all barriers).

FOR EACH SIMULATION:

1.   Data: IRANGE1   IRANGE2   HFBALG   HFBATH   HFBATV   HFBDIF

IRANGE1   Number of first barrier in range that will be assigned with following values.

IRANGE2   Number of last barrier in range that will be assigned with following values.

HFBALG   Longitudinal dispersivity for current range of barriers.

HFBATH   Transverse horizontal dispersivity for current range of barriers.

HFBATV   Transverse vertical dispersivity for current range of barriers.

HFBDIF   Diffusion coefficient for current range of barriers.

The number of the barrier is determined by the order of definition of the barriers in the HFB package input. IRANGE1 must be set equal to 1 for the first line of data. If all barrier properties are equal, set IRANGE1 = 1 and IRANGE2 = NHFB, where NHFB is the total number of barriers defined using the HFB package. If barrier properties vary, repeat Data Set 1 for as many ranges of barriers as necessary.

APPENDIX B: SELECTED ANNOTATED INPUT FILES FOR SAMPLE PROBLEM

Following are annotated copies of selected input data files used to generate the solution for the test problem using an implicit representation of the barrier on the coarse grid, with barrier dispersion properties set equal to those in the aquifer. Some of the following data files are those required for *MODFLOW* and *HFB*, and their formats are described by Harbaugh and others (2000) and Hsieh and Freckleton (1993). A complete set of input files will be available for downloading over the internet at the same site where the code is available. Some repetitive lines of input have been deleted where indicated by an ellipsis (. . .).

Following (enclosed in a border) are the contents of the *MODFLOW* name file for the sample problem; explanations are noted outside of border:

File name: *slurryc3.nam*

list	4	slurryc3.lst	← Designates main output file for *MODFLOW*
dis	7	slurryc3.dis	← Discretization input data for *MODFLOW*
bas6	8	slurryc3.bas	← Basic input data for *MODFLOW*
bcf6	10	slurryc3.bcf	← Block-centered flow package
rch	11	slurryc3.rch	← Recharge package
hfb6	12	slurryc3.hfb	← Horizontal-flow barrier package
pcg	19	slurryc3.pcg	← Input for numerical solution of flow equation
gwt	14	slurryc3.gwt	← Transport name file (turns transport "on")

↑   ↑   ↑
1   2   3

[1] Ftype (that is, the type of file)
[2] Unit number
[3] File name (name chosen to reflect contents of file)

Following (enclosed in a border) are the contents of the HFB input data file for the sample problem; explanations are noted outside of border:

File name: *slurryc3.hfb*

```
0  0  38                                          ←1
1  22  33  21  33  5.670000000000E-004            ←2
1  22  34  21  34  5.670000000000E-004            ←2
...  (SIMILAR DEFINITIONS OF 36 MORE BARRIERS FOLLOW)
```

[1] Number of HFB parameters, number of barriers defined by parameters, number of barriers
[2] Layer, two row-column pairs that define the barrier face, hydraulic conductivity of barrier divided by width of barrier

Following (enclosed in a border) are the contents of the GWT name file for the sample problem; explanations are noted outside of border:

File name: *slurryc3.gwt*

clst	15	slurryc.out	← Designates main output file for GWT Process
mocimp	16	slurryc.moc	← Main input data file for GWT
obs	21	slurryc.mob	← Input data file for observation wells
data	3	slurryc.oba	← Output file for observation well data
crch	17	slurryc.crc	← Concentrations associated with recharge
chfb	33	slurryc.chf	← CHFB package input

Following (enclosed in a border) are the contents of the CHFB input data file for the sample problem; explanations are noted outside of border:

File name: *slurryc3.chf*

```
1  38  0.5  0.025  0.0  1E-4                       ←1
```

[1] Beginning of range of barrier numbers, end of range, longitudinal dispersivity of barrier, transverse horizontal dispersivity, transverse vertical dispersivity, effective diffusion coefficient

APPENDIX C: SELECTED ANNOTATED OUTPUT FOR SAMPLE PROBLEM

This example output was generated from the input data sets listed in appendix B for the implicit case on the coarse grid with barrier dispersion properties set equal to those in the aquifer. The line spacing and font sizes of the output files have been modified in places to enhance the clarity of reproduction in this report. Some repetitive lines of output have been deleted where indicated by an ellipsis (. . .).

Some brief annotations were added in a few places in this sample output listing to help the reader understand the purpose of various sections of output. These annotations are written in bold italics to clarify that they are not part of the output file.

Following are the contents of the GWT main output file for the sample problem.

```
               U.S. GEOLOGICAL SURVEY
          Ground-Water Transport Process (GWT)
             GWT (Version 1.1) February 2002


   LISTING FILE: slurryc3.out    UNIT  15

   OPENING slurryc3.moc
   FILE TYPE:MOCIMP    UNIT  16    STATUS:OLD
   FORMAT:FORMATTED                ACCESS:SEQUENTIAL

   OPENING slurryc3.mob
   FILE TYPE:OBS    UNIT  21    STATUS:OLD
   FORMAT:FORMATTED                ACCESS:SEQUENTIAL

   OPENING slurryc3.oba
   FILE TYPE:DATA    UNIT  3    STATUS:UNKNOWN
   FORMAT:FORMATTED                ACCESS:SEQUENTIAL

   OPENING slurryc3.crc
   FILE TYPE:CRCH    UNIT  17    STATUS:OLD
   FORMAT:FORMATTED                ACCESS:SEQUENTIAL

   OPENING slurryc3.chf
   FILE TYPE:CHFB    UNIT  33    STATUS:OLD
   FORMAT:FORMATTED                ACCESS:SEQUENTIAL

   GWT BASIC INPUT READ FROM UNIT  16
```

FILE INFORMATION *(annotation)*

2 TITLE LINES:

```
Slurry wall
Coarse grid
```

PROBLEM DESCRIPTORS, INCLUDING GRID CHARACTERISTICS AND PARTICLE INFORMATION:
```
      MAPPING OF SOLUTE-TRANSPORT SUBGRID IN FLOW GRID:
   FIRST LAYER FOR SOLUTE TRANSPORT =   1    LAST LAYER FOR SOLUTE TRANSPORT  =    1
   FIRST ROW FOR SOLUTE TRANSPORT   =   7    LAST ROW FOR SOLUTE TRANSPORT    =   23
   FIRST COLUMN FOR SOLUTE TRANSPORT=  31    LAST COLUMN FOR SOLUTE TRANSPORT =   43

   UNIFORM DELCOL AND DELROW IN SUBGRID FOR SOLUTE TRANSPORT
```

```
NO. OF LAYERS =    1   NO. OF ROWS =    17   NO. OF COLUMNS =    13
NO SOLUTE DECAY
MOLECULAR DIFFUSION CONSTANT, DIFFUS=1.00000E-10
MAXIMUM NUMBER OF PARTICLES (NPMAX) =   1000000
  4010353 ELEMENTS IN X ARRAY ARE USED BY GWT
  1012912 ELEMENTS IN IX ARRAY ARE USED BY GWT


CRCH5  --  CONCENTRATIONS IN RECHARGE INPUT READ FROM UNIT  17
       221 ELEMENTS IN X ARRAY ARE USED BY RCH
        12 ELEMENTS IN X ARRAY ARE USED BY OBS
```

```
CHFB: NUMBER OF BARRIERS =    38
 HFB RANGE:    1 TO   38
   LONGITUDINAL DISPERSIVITY =      5.0000E+00
   TRANSVERSE HORIZ DISP     =      2.5000E-01
   TRANSVERSE VERT DISP      =      0.0000E+00
   DIFFUSION COEFFICIENT     =      1.0000E-04
```
CHFB

PACKAGE

```
NUMBER OF PARTICLES INITIALLY IN EACH ACTIVE CELL (NPTPND) =   -696
 READ IN NONSTANDARD INITIAL PARTICLE COORDINATES


INITIAL RELATIVE PARTICLE COORDINATES
   IP     PNEWL       PNEWR       PNEWC
    1    0.00000     0.00000    -0.49000
    2    0.00000     0.00000    -0.48000
    3    0.00000     0.00000    -0.47000


  . . .


  694    0.00000     0.47000     0.00000
  695    0.00000     0.48000     0.00000
  696    0.00000     0.49000     0.00000


  CELDIS=      1.000000
   FZERO=      0.00015

INTRPL= 1:  LINEAR INTERPOLATION SCHEME

NUMERICAL PARAMETERS FOR IMPLICIT SOLVER:
FDTMTH =      1.00
NCXIT  =      2
IDIREC =      1
EPSSLV =  1.0000E-05
MAXIT  =    100
```

```
NPNTCL=     0:      CONCENTRATIONS WILL BE WRITTEN AT THE END OF THE SIMULATION
MODFLOW FORMAT SPECIFIER FOR CONCENTRATION DATA: ICONFM=     0

NPNTVL=    -1:             VELOCITIES WILL BE WRITTEN AT THE END OF EVERY STRESS
PERIOD
MODFLOW FORMAT SPECIFIER FOR       VELOCITY DATA: IVELFM=     0

NPNTDL=     0: DISP. COEFFICIENTS WILL NOT BE WRITTEN

NPNTPL=     0: PARTICLE LOCATIONS WILL BE WRITTEN AT THE END OF THE SIMULATION
```
OUTPUT

CONTROL

```
CONCENTRATION WILL BE SET TO -999.90     AT ALL NO-FLOW NODES (IBOUND=0).

             INITIAL CONCENTRATION FOR LAYER    1
  READING ON UNIT   16 WITH FORMAT: (FREE)

          1       2       3       4       5       6       7       8       9      10
         11      12      13
 ........................................................................................
  1    0.000   0.000   0.000   0.000   0.000   0.000   0.000   0.000   0.000   0.000
       0.000   0.000   0.000
  2    0.000   0.000   0.000   0.000   0.000   0.000   0.000   0.000   0.000   0.000
       0.000   0.000   0.000
  3    0.000   0.000   100.0   100.0   100.0   100.0   100.0   100.0   0.000   0.000
       0.000   0.000   0.000
  4    0.000   0.000   100.0   100.0   100.0   100.0   100.0   100.0   0.000   0.000
       0.000   0.000   0.000
  5    0.000   0.000   100.0   100.0   100.0   100.0   100.0   100.0   0.000   0.000
       0.000   0.000   0.000

 . . .
```

VALUES OF C' REQUIRED FOR SUBGRID BOUNDARY ARRAY =   1
ONE FOR EACH LAYER IN TRANSPORT SUBGRID

ORDER OF C' VALUES: FIRST LAYER IN SUBGRID, EACH SUBSEQUENT LAYER,
LAYER ABOVE SUBGRID, LAYER BELOW SUBGRID:

            SUBGRID BOUNDARY ARRAY
READING ON UNIT 16 WITH FORMAT: (FREE)
   0.0000

NUMBER OF ZONES FOR CONCENTRATIONS AT FIXED HEAD CELLS =   1

ZONE FLAG =   -1   INFLOW CONCENTRATION =   0.0000E+00

                    SINK-SOURCE FLAG FOR LAYER   1
READING ON UNIT 16 WITH FORMAT: (FREE)

IGENPT ARRAY

	1	2	3	4	5	6	7	8	9	10	11	12	13
1	0	0	0	0	0	0	0	0	1	0	1	0	0
2	0	0	0	0	0	0	0	0	0	0	0	0	0
3	0	0	0	0	0	0	0	0	0	0	0	0	0
4	1	0	0	0	0	0	0	0	0	0	0	0	0
5	0	0	0	0	0	0	0	0	0	0	0	0	0
6	1	0	0	0	0	0	0	0	0	0	0	0	0
7	0	0	0	0	0	0	0	0	0	0	0	0	0
8	0	0	0	0	0	0	0	0	0	1	0	0	0
9	0	0	0	0	0	0	0	0	1	1	0	0	0
10	0	0	0	0	0	0	0	0	0	1	0	0	0
11	0	0	0	0	0	0	0	0	0	0	0	0	0
12	1	0	0	0	0	0	0	0	0	0	0	0	0
13	0	0	0	0	0	0	0	0	0	0	0	0	0
14	1	0	0	0	0	0	0	0	0	0	0	0	0
15	0	0	0	0	0	0	0	0	0	0	0	0	0
16	0	0	0	0	0	0	0	0	0	0	0	0	0
17	0	0	0	0	0	0	0	0	1	0	1	0	0

            LONGITUDNL. DISPERSIVITY
READING ON UNIT 16 WITH FORMAT: (FREE)
   5.0000

            HORIZ. TRANSVERSE DISP.
READING ON UNIT 16 WITH FORMAT: (FREE)
   0.25000

            VERT. TRANSVERSE DISP.
READING ON UNIT 16 WITH FORMAT: (FREE)
   0.0000

            RETARDATION FACTOR
READING ON UNIT 16 WITH FORMAT: (FREE)
   1.0000

INITIAL POROSITY = 0.300000 FOR LAYER   1

COORDINATES FOR   3 OBSERVATION WELLS:

WELL #	LAYER	ROW	COLUMN	UNIT
1	1	14	40	3
2	1	15	39	3
3	1	15	41	3

ALL OBSERVATION WELL DATA WILL BE WRITTEN ON UNIT   3

```
SATURATED THICKNESS, SUBGRID LAYER          1
-----------------------------------------------
   21.45632       21.40205       21.33396       21.26428       21.19453
   21.12405       21.05186       20.97729       20.90203       20.83976
   20.78578       20.73606       20.68834
   21.48417       21.43328       21.34576       21.26893       21.19568
   21.12247       21.04656       20.96414       20.86728       20.80862
   20.76071       20.71608       20.67230
   . . .
   21.12406       21.05186       20.97729       20.90204       20.83976
   20.78578       20.73606       20.68834
```

```
TOTAL NUMBER OF PARTICLES GENERATED =      155828
TOTAL NUMBER OF ACTIVE NODES (NACTIV) =        221
MAX. NUMBER OF CELLS THAT CAN BE VOID OF PARTICLES (NZCRIT) =        0
    (IF NZCRIT EXCEEDED, PARTICLES ARE REGENERATED)
```

```
                        CONC. IN RECHARGE
READING ON UNIT  17 WITH FORMAT: (FREE)

        1        2        3        4        5        6        7        8        9       10
       11       12       13
...........................................................................................
 1   0.000    0.000    0.000    0.000    0.000    0.000    0.000    0.000    0.000    0.000
     0.000    0.000    0.000
 2   0.000    0.000    0.000    0.000    0.000    0.000    0.000    0.000    0.000    0.000
     0.000    0.000    0.000
 3   0.000    0.000    0.000    0.000    0.000    0.000    0.000    0.000    0.000    0.000
     0.000    0.000    0.000
. . .
```

```
          STABILITY CRITERIA --- M.O.C.

  MAXIMUM FLUID VELOCITIES: C-VEL =  6.12E-01     R-VEL =  4.69E-01     L-VEL =  4.44E-23
  MINIMUM TIME TO TRAVEL THCK =   2.25E+22

TIMV =  2.45E+01     NTIMV  =     204

    MAX. C-VEL. IS CONSTRAINT AND OCCURS BETWEEN NODES (  39,  22,   1) AND (  38,  22,   1)

MAXIMUM INJECTION OCCURS IN J,I,K=  43  15   1

TMV  =  2.71E+03     NTIMIJ =        1


NUMBER OF MOVES FOR ALL STABILITY CRITERIA:
   CELDIS    INJECTION
     204           1

CELDIS IS LIMITING
          TIME STEP     1 IN STRESS PERIOD     1

          NO. OF PARTICLE MOVES REQUIRED TO COMPLETE THIS TIME STEP  =  204
             MOVE TIME STEP (TIMV)=  2.450980377197E+01
```

(NUMERICAL SOLUTION TO TRANSPORT EQUATION STARTS AT THIS POINT)

```
  NP       =      155828 AT START OF MOVE          IMOV     =             1
  No. of solver iterations =     2 Relative residual =   6.8656E-08
  NP       =      157115 AT START OF MOVE          IMOV     =             2
  No. of solver iterations =     2 Relative residual =   7.3278E-08
. . .
  NP       =      167741 AT START OF MOVE          IMOV     =           203
  No. of solver iterations =     2 Relative residual =   1.0595E-07
  NP       =      169248 AT START OF MOVE          IMOV     =           204
```

CONCENTRATIONS: SUBGRID LAYER   1 = MODFLOW LAYER   1
AT END OF TRANSPORT TIME INCREMENT   204 IN TIME STEP   1 IN STRESS PERIOD 1

| | 1 | 2 | 3 | 4 | 5 | 6 | 7 | 8 | 9 | 10 |
	11	12	13							
1	1.3041E-02	3.8899E-02	8.5495E-02	0.1396	0.1609	0.1845	0.1931	0.1716	0.1845	0.1840
	0.1881	0.1996	0.2003							
2	5.4278E-02	0.2944	0.7102	0.7883	0.9610	1.219	1.319	1.298	0.8635	0.3046
	0.2293	0.2052	0.1996							
3	0.1930	0.7846	9.599	24.23	28.29	28.42	26.28	12.23	1.693	0.8011
	0.3529	0.2914	0.2399							
4	0.2461	0.8521	48.13	91.54	98.76	99.50	97.61	57.74	2.001	1.387
	0.8861	0.4352	0.3765							
5	0.2255	0.8336	55.65	93.24	99.34	99.90	98.46	67.98	2.801	1.691
	1.319	0.9635	0.6093							
6	0.2064	0.9767	62.66	94.44	99.47	99.93	98.91	76.93	3.776	2.404
	1.716	1.296	1.043							
7	0.1171	0.7777	67.78	95.32	99.56	99.95	99.31	85.17	5.963	3.667
	2.860	1.966	1.791							
8	9.5219E-02	0.7992	74.88	96.44	99.67	99.97	99.64	92.34	9.511	6.795
	6.327	4.933	4.076							
9	8.2489E-02	0.8395	75.61	96.55	99.68	99.97	99.65	92.64	11.98	10.06
	9.453	8.028	7.404							
10	9.5216E-02	0.7991	74.89	96.44	99.67	99.97	99.64	92.34	9.507	6.792
	6.324	4.931	4.074							
11	0.1170	0.7776	67.78	95.32	99.56	99.95	99.31	85.17	5.962	3.666
	2.860	1.966	1.791							
12	0.2063	0.9765	62.66	94.44	99.47	99.93	98.91	76.93	3.776	2.404
	1.716	1.296	1.044							
13	0.2254	0.8334	55.65	93.24	99.34	99.90	98.46	67.98	2.801	1.691
	1.319	0.9634	0.6094							
14	0.2461	0.8519	48.13	91.53	98.75	99.50	97.61	57.73	2.001	1.387
	0.8852	0.4351	0.3764							
15	0.1930	0.7841	9.501	24.06	28.20	28.45	26.43	12.34	1.692	0.8008
	0.3527	0.2912	0.2398							
16	5.4207E-02	0.2940	0.7095	0.7874	0.9599	1.218	1.318	1.296	0.8633	0.3044
	0.2291	0.2050	0.1994							
17	1.3014E-02	3.8851E-02	8.5347E-02	0.1394	0.1606	0.1843	0.1928	0.1713	0.1843	0.1839
	0.1879	0.1993	0.2000							

SOLUTE BUDGET AND MASS BALANCE FOR TRANSPORT SUBGRID

VALUES CALCULATED AT END OF:
    STRESS PERIOD   1 OUT OF   1
    FLOW TIME STEP   1 OUT OF   1
TRANSPORT TIME INCREMENT   204 OUT OF   204

ELAPSED TIME =   5.0000E+03

CHEMICAL MASS IN STORAGE:
  INITIAL: MASS DISSOLVED = 1.1135E+07   MASS SORBED = 0.0000E+00
  PRESENT: MASS DISSOLVED = 9.0610E+06   MASS SORBED = 0.0000E+00

CHANGE IN MASS STORED =   2.0744E+06

ITEMIZED

BUDGETS FOR

SOLUTE FLUXES

CUMULATIVE SOLUTE MASS   (L**3)(M/VOL)

IN:

              DECAY = 0.0000E+00
      CONSTANT HEAD = 0.0000E+00
   SUBGRID BOUNDARY = 0.0000E+00
         RECHARGE = 0.0000E+00
            WELLS = 0.0000E+00
           RIVERS = 0.0000E+00
          DRAINS = 0.0000E+00
GENL. HEAD-DEP. BDYS. = 0.0000E+00
  EVAPOTRANSPIRATION = 0.0000E+00
 SPECIFIED FLOW (FHB) = 0.0000E+00

        TOTAL IN = 0.0000E+00

```
            OUT:
            ----
                      DECAY =   0.0000E+00
              CONSTANT HEAD =   0.0000E+00
          SUBGRID BOUNDARY = -2.8362E+06
                  RECHARGE =   0.0000E+00
                     WELLS =   0.0000E+00
                    RIVERS =   0.0000E+00
                    DRAINS =   0.0000E+00
     GENL. HEAD-DEP. BDYS. =   0.0000E+00
        EVAPOTRANSPIRATION =   0.0000E+00
      SPECIFIED FLOW (FHB) =   0.0000E+00

                 TOTAL OUT = -2.8362E+06


        SOURCE-TERM DECAY =   0.0000E+00



                  RESIDUAL = -7.6174E+05

   PERCENT DISCREPANCY =   2.6858E+01 RELATIVE TO MASS FLUX OUT

   PERCENT DISCREPANCY = -8.4068E+00 RELATIVE TO INITIAL MASS STORED
```